Int. J. Electrochem. Sci., 15 **(2020)** 223 – 230, doi: 10.20964/2020.01.33

International Journal of
ELECTROCHEMICAL
SCIENCE
www.electrochemsci.org

Short Communication

Substitution Effect in Tungstovanadosilicate Ionic Liquid Gels Electrolytes

Zeqing Wang[1], *Limei Ai*[1], *Xiaoshu Lv*[1], *Zijing Wang*[1], *Fengwei He*[1], *Qingyin Wu*[1,2,*]

[1] School of Biomedical and Chemical Engineering, Liaoning Institute of Science and Technology, Benxi 117004, Liaoning, P. R. China
[2] Department of Chemistry, Zhejiang University, Hangzhou, 310027, P. R. China
[*]E-mail: qywu@zju.edu.cn

Received: 6 September 2019 / *Accepted:* 19 October 2019 / *Published:* 30 November 2019

A series of polyoxometalate-based ionic liquids (POM-ILs) electrolytes has been synthesized by self-assembly from a heteropoly acid $H_7SiW_9V_3O_{40}$ and N-methyl imidazolium-1-(3-sulfonic) propyl (MIMPS). The POM-ILs electrolytes were characterized by FTIR, UV and XRD, and the results reveal that the POM-ILs electrolytes possess a typical polyoxometalate-based ionic liquid structure. Furthermore, the substitution effect of these compounds has been investigated. The thermostability and conductivity of the POM-ILs electrolytes increased with the number of protons in compounds increased.

Keywords: Substitution effect, polyoxometalates, gels electrolytes, heteropoly acid, conductivity.

1. INTRODUCTION

Ionic liquid (IL) is a series of specific salt which remain liquid phase at low temperature or at room temperature [1,2]. Ionic liquid can be prepared through a self-assembly method for anions and cations [3,4]. Ionic liquid exhibits a remarkable thermal stability property, and significant advantages in electrochemical applications [5-7]. Gel-type ionic liquid can be obtained through noncovalent interaction and the gel still maintains the characteristic of ionic liquid (i.e., solvent ability and ionic conductivity. These gel-type ionic liquids can be classified as excellent soft materials due to perfect characteristic than traditional ionic liquid.

Polyoxometalates (POMs) or heteropoly-acids (HPA) are a series of metal oxide cluster [8-10]. The emphasis type of heteropoly acids is Keggin and Dawson.Keggin-type HPA generally has some excellent characteristics, for example stable chemical structure and/or high yield, accordingly the research of Keggin-type of heteropoly acids were widely [11-18].

Recently, researcher found that POM-based inorganic-organic hybrid compounds, which show more perfect characteristic that the pure heteropoly acids due to their unique structure and characteristic [19-23]. These materials exhibit excellent conductivity and reversible phase transformation characteristics [24-26]. Consequently, the POM-based inorganic-organic hybrid compounds have higher ionic conductivities as compared with other solid conductors, and they will be new potential candidates in current electrochemical apparatus[27, 28].

Herein, it is reported in our work that two novel inorganic-organic hybrid compounds which were synthesized by an organic ionic liquid such as N-methyl imidazolium-1-(3-sulfonic) propyl (which is called as MIMPS) and inorganic HPA such as $H_7SiW_9V_3O_{40}$. The compounds exhibit good conductivity. Furthermore, we investigate the relationship between the characteristic and the structure of conductivity and thermo-stability. The results show that proton substitution effect plays an important role.

2. EXPERIMENTAL SECTION

2.1 Synthesis of HPA

$Na_{10}[\alpha\text{-}SiW_9O_{34}]$ was prepared by a method mentioned in recent documents[28]. A 10 mL sodium metavanadate (1.71g $NaVO_3$) aqueous solution was added to a 30 mL $Na_{10}[\alpha\text{-}SiW_9O_{34}]$ (10 g $Na_{10}[\alpha\text{-}SiW_9O_{34}]$) aqueous solution, and then controlled to pH=1.5. Then the mixed liquor was added dropwise to an exchange resin column of H^+ type cations until the mixed liquor has a pH value less than 1, and then dried at about 40 °C, accordingly HPA structured as $H_7SiW_9V_3O_{40}$ was obtained.

2.2 Synthesis of POM-ILs

$[MIMPS]_3H_4SiW_9V_3O_{40}$ and $[MIMPS]_5H_2SiW_9V_3O_{40}$.was prepared by following method. The pre-synthesized MIMPS [23] and HPA were mixed in 5:1 and 3:1 molar ratios. An $H_7SiW_9V_3O_{40}$ aqueous solution was added with the MIMPS, and then the mixture was sonicated for 10 minutes at room temperature, and then lower liquid was obtained by a separatory funnel from the mixture. The obtained liquid was volatillized at room temperature, thereby products as oily matter were obtained.

2.3 Instruments and reagents

IR spectra were collected by NICOLET NEXUS 470 FT/IR spectrometer at 400–4000 cm^{-1}. XRD patterns were collected by BRUKER D8 ADVANCE X-ray diffractometer in the range of 2θ = 4-40° at a rate of $0.02°\cdot s^{-1}$. The thermal stability was collected by SHIMADZU thermal analyzer in the range of 25-500 °C at a rate of 10 $°C\cdot min^{-1}$. The UV absorption spectra of $H_7SiW_9V_3O_{40}$, $[MIMPS]_3H_4SiW_9V_3O_{40}$ and $[MIMPS]_5H_2SiW_9V_3O_{40}$ were collected by Specord TU-1901 UV-Vis spectrophotometer. Conductivity were collected by DDS-11A conductivity meter using a Shanghai DJS-10 electrode which electrode constant k is 9.42.

All reagents were of analytical grade.

3. RESULTS AND DISCUSSION

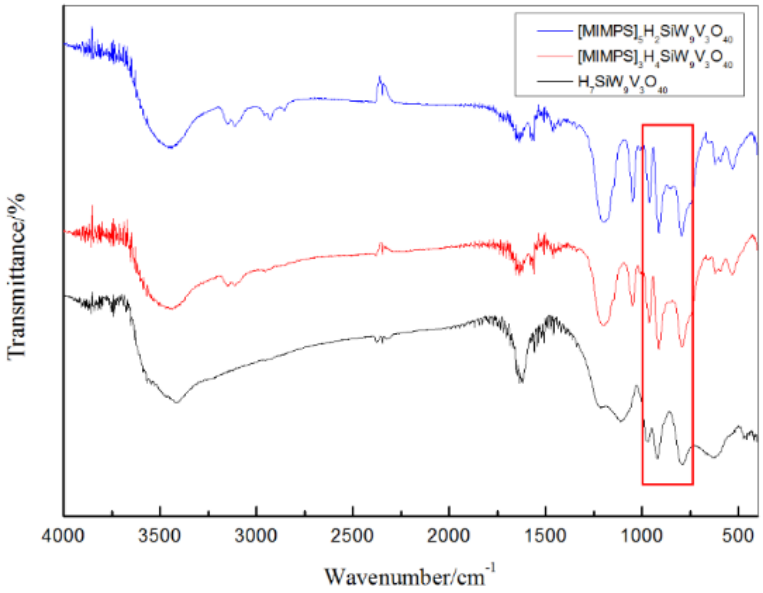

Figure 1. IR spectra of $H_7SiW_9V_3O_{40}$, $[MIMPS]_3H_4SiW_9V_3O_{40}$ and $[MIMPS]_5H_2SiW_9V_3O_{40}$.

Table 1. The IR spectra of compounds in the range of 1100~700 cm^{-1}

Vibrations /cm^{-1}	SiW_9V_3	$[MIMPS]_3H_4SiW_9V_3$	$[MIMPS]_5H_2SiW_9V_3$
M-O_d stretching	970	963	961
Si-O_a stretching	916	911	911
M-O_b-M stretching	-	-	-
M-O_c-M stretching	786	792	795
S=O dending	-	1210	1221
S=O dending	-	1164	1173
O-H stretching	3461	3457	3450
H-O-H bending	1623	1635	1640

The IR spectra of samples in the range of 4000~400 cm^{-1} are illustrated in Fig. 1 and the detail IR spectra of samples can be found in Table 1. Many feature frequencies can be found in Fig. 1 and Table 1. The feature frequencies of all samples fall in the stretching sequence of ν_{as}(M-O_b-M), ν_{as}(M-O_d), ν_{as}(M-O_c-M) andν_{as}(Si-O_a), (M=W, V), which are referred to POM vibration bands at 1100~700 cm^{-1}. It is further observed that the characteristic peaks of POM-ILs are slightly shifted when compared with vibration band of HPA in Fig. 1 and Table 1. This phenomenon can be resulted in the influence of the anion-anion interactions [24]. Furthermore, additional characteristic peaks at 1210 cm^{-1}, 2960 cm^{-1} are assigned to $\nu_{S=O}$ and ν_{C-H}, respectively. Although the characteristic peaks of POM-ILs exhibit shift, the characteristic peaks of POM still exist (red frame zone in Fig. 1). This results

indicate that POM structure still was maintained even if MIMPS are added. UV absorption spectra of samples are illustrated in Fig. 2.

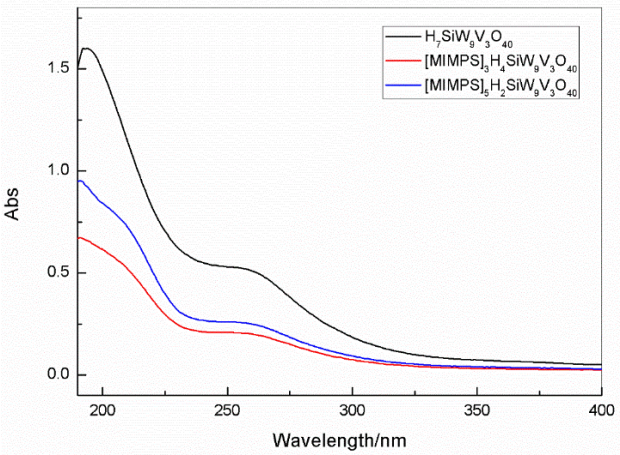

Figure 2. UV absorption spectra of the compounds.

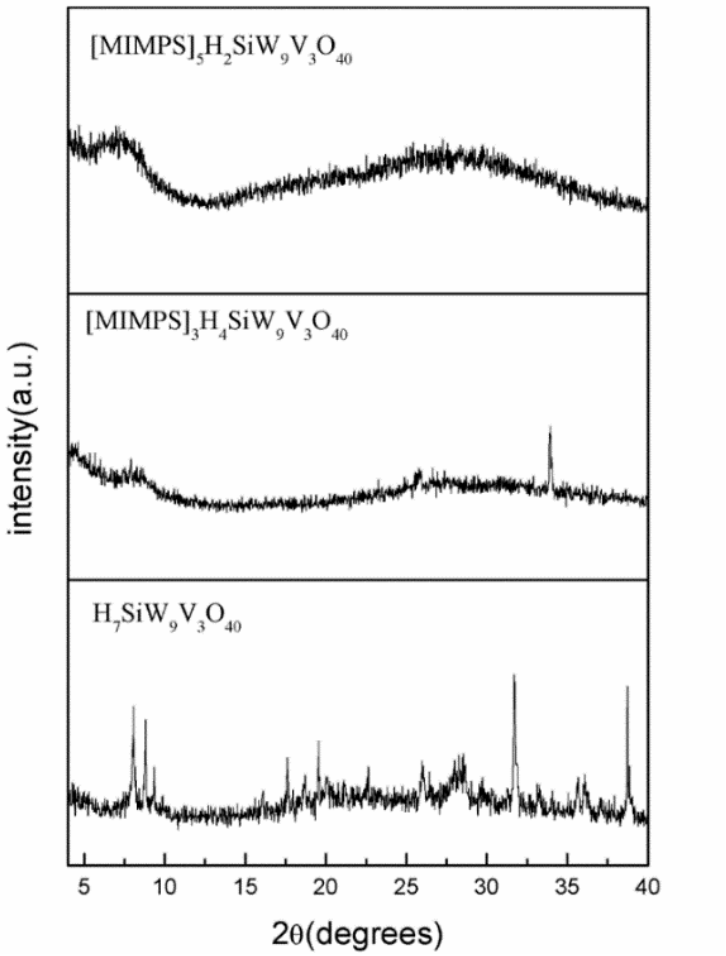

Figure 3. Wide-angle XRD patterns of the compounds.

It can be found from Fig. 2 that the absorption spectra of POM-ILs show a moderately intensity peak nearly 258 nm since a bridge-oxygen (O_b, O_c) is charge-transferred toward metal atoms in the

heteropolyanion cage [27]. Furthermore, the blue-shifted phenomenon of peak was observed nearly 260 nm, which is called as the pure POM. The phenomenon as described above can infer that it exists an intermolecular interactions between POM anion and organic cations (MIMPS) units [27].

Wide-angle XRD patterns for the samples and HPA are illustratedin Fig. 3. There are some strong peaks in the XRD patterns of $H_7SiW_9V_3O_{40}$. Phase and structure information were collected by XRD and the results were shown in Fig. 3. Typical peaks of keggin-type of the polyoxometalates were found in the range of 2θ=7-10° from the XRD patterns. This result can provide a proof that the POM-ILs were successfully prepared [23]. Furthermore, a broad diffraction peaks occurred at 2θ=20-35° of POM-ILs, which is consistent with amorphous structure. It is suggest that the HPA was transformed to an amorphous structure after adding MIMPS. The results means that the arrangement of HPA is rearranged after adding MIMPS, and the schematic illustration of interactions among MIMPS, protons and POM anion is shown in Fig. 4.

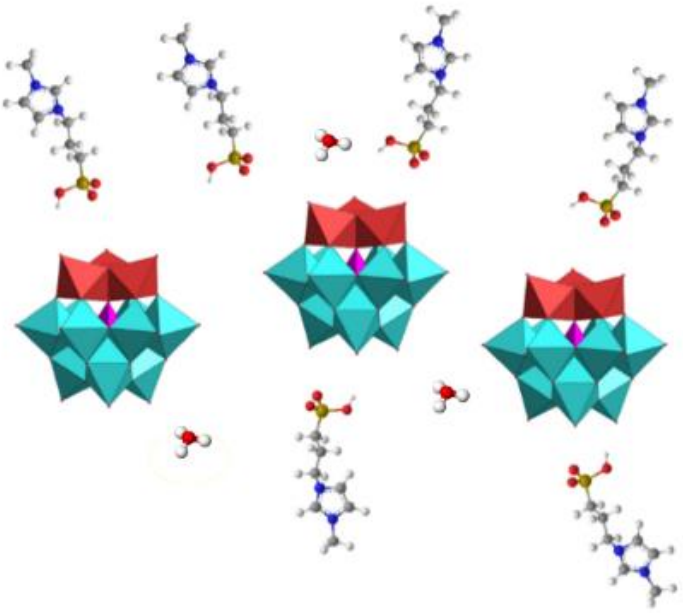

Figure 4. Schematic structural illustration of POM-LIs.

The thermal stability characterization of POM-ILs can be analyzed by the exothermic peak on the DTA or DSC [29] and the results are shown in table 2. Melting point can be found in DSC result and melting point of $[MIMPS]_3H_4SiW_9V_3O_{40}$ and $[MIMPS]_5H_2SiW_9V_3O_{40}$ are 106 °C and 100 °C respectively. We can also thermal decomposition at 300-400 °C. Thermal decomposition temperature of $[MIMPS]_3H_4SiW_9V_3O_{40}$ and $[MIMPS]_5H_2SiW_9V_3O_{40}$ are 371 °C and 321 °C, respectively. This phenomenon is due to the decomposition of MIMPS. The results exhibit that the thermal stability of POM-IL is excellent and thermal stability is changed to poor with increasing of the mount of MIMPS in POM-IL compounds.

Table 2. Temperature of exothermic and endothermic peak in DSC.

	Endo-peak /°C	Exo-peak /°C
$[MIMPS]_3H_4SiW_9V_3O_{40}$	100	371
$[MIMPS]_5H_2SiW_9V_3O_{40}$	106	321

The change of the conductivity with increasing of temperature among the POM-ILs was showed in Fig.5. The conductivity of $[MIMPS]_5H_2SiW_9V_3O_{40}$ and $[MIMPS]_3H_4SiW_9V_3O_{40}$ is 1.3×10^{-2} $S\cdot cm^{-1}$ and 1.9×10^{-2} $S\cdot cm^{-1}$, respectively. Fig.5 depicts conductivity of compounds decrease with the increase of amount of MIMPS substitution at same temperature. In other words, conductivity is positively correlated with the number of protons. This result can be explained as the migration rate of protons faster than MIMPS. And then, numerous protons will lead to a high conductivity [30].

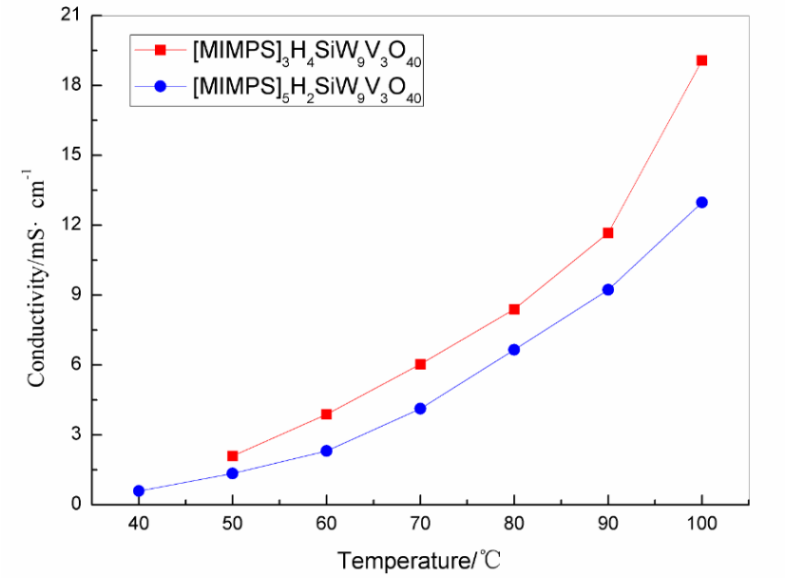

Figure 5. Temperature-conductivity curves of $[MIMPS]_5H_2SiW_9V_3O_{40}$, and $[MIMPS]_3H_4SiW_9V_3O_{40}$.

The conductive activation energy E_a can be calculated as follow

$$\sigma = \sigma_0 exp\left(\frac{-E_a}{RT}\right)$$

Wherein σ represents the conductivity of the sample, σ_0 represents the pre-exponential factor, E_a represents the conductive activation energy, R represents the gas constant, and T represents the absolute temperature. Conductive Arrhenius plots of $[MIMPS]_5H_2SiW_9V_3O_{40}$ and $[MIMPS]_3H_4SiW_9V_3O_{40}$ at the same condition as shown in Fig.6. E_a of $[MIMPS]_5H_2SiW_9V_3O_{40}$ and $[MIMPS]_3H_4SiW_9V_3O_{40}$ respectively are 42.17 $kJ\cdot mol^{-1}$ and 37.76 $kJ\cdot mol^{-1}$. These results infer that the substitution effect of the protons in these compounds is obviously which can be confirmed by lower conductive activation energy[25].

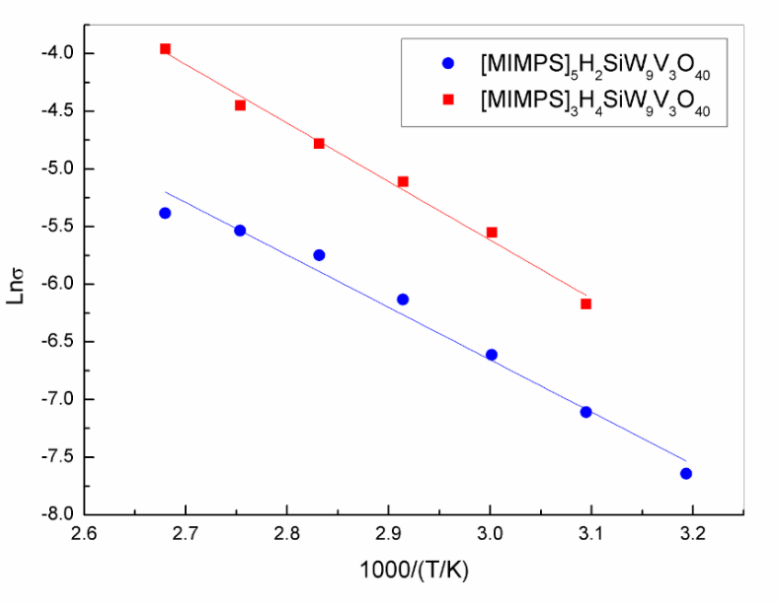

Figure 6. Conductive Arrhenius plots of $[MIMPS]_3H_4SiW_9V_3O_{40}$ and $[MIMPS]_5H_2SiW_9V_3O_{40}$.

4. CONCLUSIONS

In this work, two novel polyoxometalate-based ionic liquid electrolytes have been successfully synthesized by using MIMPS ionic liquid, and the substitution effect for these compounds have been researched. With the protons replace the MIMPS into the structure, the compounds exhibit higher conductivity and better thermostability.

ACKNOWLEDGEMENTS
The study was financially supported by the project of Liaoning Provincial Natural Science Foundation of China (No. 201602404), the Zhejiang Provincial Natural Science Foundation of China (No. LY18B010001) and PhD Research Startup Foundation of Liaoning Institute of Science and Technology (No. 1810B08).

References

1. B. P. Mudraboyina, M. M. Obadia, I. Allaoua, R. Sood, A. Serghei and E. Drockenmuller, *Chem. Mater.*, 26 (2014) 1720.
2. J. F. Ping, Y. X. Wang, Y. B. Ying and J. Wu, *RSC Adv.*, 3 (2013) 19782.
3. N. N. Lei, S. J. Yi, J. Wang, Q. T. Li and X. Chen, *J. Phys. Chem. B*, 121 (2017) 11528.
4. K. Shakeela, V. L. Sinduri and G. R. Rao, *Polyhedron*, 137 (2017) 43.
5. S. Tan, G. A. Baker and H. Zhao, *Chem. Soc. Rev.*, 41 (2012) 4030.
6. C. Yao, Q. Lu, X. H. Wang and F. S. Wang, *J. Phys. Chem. B*, 118 (2014) 4661.
7. J. S. Yan, Z. Q. Wang, Y. S. E, F. W. He, D. F. Zhang and Q. Y. Wu, *RSC Adv.*, 9 (2019) 8404.
8. J. Miao, Z. l. Lang, X. Y. Zhang, W. G. Kong, O. W. Peng, Y. Yang, S. P. Wang, J. J. Cheng, T. C. He, A. Amini, Q. Y. Wu, Z. P. Zheng, Z. K. Tang and C. Cheng, *Adv. Funct. Mater.*, 28 (2019)

1805893.
9. M. Bonchio, Z. Syrgiannis, M. Burian, N. Marino, E. Pizzolato, K. Dirian, F. Rigodanza, G. A. Volpato, G. La Ganga, N. Demitri, S. Berardi, H. Amenitsch, D. M.Guldi, S. Caramori, C. A. Bignozzi, A. Sartorel and M. Prato, *Nat. Chem.*, 11 (2019) 146.
10. H. X. Cai, X. F. Wu, Q. Y. Wu and W. F. Yan, *Dalton Trans.*, 45 (2016) 14238.
11. H. Wu, X. F. Wu, Q. Y. Wu and W. F. Yan, *Compos. Sci. Technol.*, 162 (2018) 1.
12. L. M. Ai, D. F. Zhang, Q. Wang, J. S. Yan and Q. Y. Wu, *Catal. Commun.*, 126 (2019) 10.
13. W. S. Dai, X. Tong and Q. Y. Wu, *Int. J. Electrochem. Sci.*, 14 (2019) 8931.
14. Z. Zheng, Q. J. Zhou, M. Li and P. C. Yin, *Chem. Sci.*, 10 (2019) 7333.
15. F. M. Santos, S. P. Magina, H. I. S. Nogueira and A. M. V. Cavaleiro, *New J. Chem.*, 40 (2016) 945.
16. K. Kamata1, K. Yonehara, Y. Sumida, K. Yamaguchi, S. Hikichi and N. Mizuno, *Science*, 300 (2003) 964.
17. H. B. Liu, L. Bai, L. M. Ai, W. S. Dai, D. F. Zhang, Q. Y. Wu and R. C. Zhang, *J. Rare Earth.*, 37 (2019) 617.
18. Y. Leng, C. J. Zhang, B. Liu, M. M. Liu, P. P. Jiang and S. Dai, *ChemSusChem*, 11 (2018) 3396.
19. A. Misra, I. F. Castillo, D. P. Müller, C. González, S. Eyssautier-Chuine, A. Ziegler, J. M. Fuente, S. G. Mitchell and C. Streb, *Angew. Chem. Int. Ed.*, 57 (2018) 14926.
20. Q. Y. Wu, X. Y. Qian and S. M. Zhou, *J. Xuzhou Inst. Tech. (Nat. Sci. Ed.)*, 27 (2012) 1.
21. S. Herrmann, L. De Matteis, J. M. Fuente, S. G. Mitchell and C. Streb, *Angew. Chem. Int. Ed.*, 56 (2017) 1667.
22. T. Ueda, K. Kodani, H. Ota, M. Shiro, S. X. Guo, J. F. Boas and A. M. Bond, *Inorg. Chem.*, 56 (2017) 3990.
23. X. F. Wu, X. Tong, Q. Y. Wu, H. Ding and W. F. Yan, *J. Mater. Chem. A*, 2 (2014) 578.
24. Y. Y. Li, X. F. Wu, Q. Y. Wu, H. Ding and W. F. Yan, *Dalton Trans.*, 43 (2014) 13591.
25. X. F. Wu, W. Wu, Q. Y. Wu and W. F. Yan, *Langmuir*, 33 (2017) 4242.
26. Z. R. Xie, Q. Y. Wu, W. S. Dai and F. W. He, *Int. J. Electrochem. Sci.*, 13 (2018) 11684.
27. T. P. Huang, N. Q. Tian, Q. Y. Wu and W. F. Yan, *Soft Matter*, 11 (2015) 4481.
28. Z. R. Xie, H.Wu, Q.Y. Wu and L. M. Ai, *RSC Adv.*, 8 (2018) 13984.
29. Q. Y. Wu, X. Q. Cai, W. Q. Feng and W. Q. Pang, *Thermochim. Acta*, 428 (2005) 15.
30. T. L. Greaves and C. J. Drummond, *Chem. Rev.*, 115 (2015) 11379.